RACK1 may participate in placental development via regulating proliferation and migration of trophoblast cell in pigs following intrauterine growth restriction

Zhimin Wu[1,2], Guangling Hu[1,2], Ting Gong[1,2], Qun Hu[3], Linjun Hong[3], Yiyu Zhang[1,2], Zheng Ao[1,2,*]

[1] Key Laboratory of Animal Genetics, Breeding and Reproduction in the Plateau Mountainous Region, Ministry of Education, College of Animal Science, Guizhou University, Guiyang, China.

[2] Guizhou Provincial Key Laboratory of Animal Genetics, Breeding and Reproduction, College of Animal Science, Guizhou University, Guiyang, China.

[3]National Engineering Research Center for Breeding Swine Industry, College of Animal Science, South China Agricultural University, Guangzhou, Guangdong, China.

* Corresponding author: E-mail addresses: zao@gzu.edu.cn (ZA);

Abstract: Intrauterine growth restriction (IUGR) is a severe complication in swine production. Placental insufficiency is responsible for inadequate fetal growth, but the specific etiology of placental dysfunction-induced IUGR in pigs remains poorly understood. In this work, placenta samples supplying the lightest-weight (LW) and mean-weight (MW) pig fetuses in the litter at day 65 (D65) of gestation were collected, and the relationship between fetal growth and placental morphologies and functions was investigated using histomorphological analysis, RNA sequencing, quantitative polymerase chain reaction, and in-vitro experiment in LW and MW placentas. Results showed that the folded structure of the epithelial bilayer of LW placentas followed a poor and incomplete development compared with that of MW placentas. A total of 632 differentially expressed genes (DEGs) were screened out between the LW and MW placentas, and RACK1 was found to be downregulated in LW placentas. The DEGs were mainly enriched in translation, ribosome, protein synthesis, and mTOR signaling pathway according to GO and KEGG enrichment analyses. In-vitro experiments indicated that the decreased RACK1 in LW placentas may be involved in abnormal development of placental folds (PFs) by inhibiting the proliferation and migration of porcine trophoblast cells. Taken together, these results revealed that RACK1 may be a vital regulator in the development of PFs via regulating trophoblast ribosome function, proliferation, and migration in pigs.

Keywords: RACK1; Placenta; Pig; ribosome; trophoblast cell

1 Introduction

Intrauterine growth restriction (IUGR) is a common obstetrical complication resulting in many adverse effects on fetal growth and development and postnatal health [1, 2]. Pigs are one of multiparous species most likely to suffer from IUGR among domestic animals (accounting

for 15%–25% of births), though a good deal of measures has been made to reduce the occurrence of IUGR, which negatively influences the production performance and economic benefits of pig production [3] . Piglets with IUGR have been shown to be followed by high morbidity and mortality, and they are predisposed to stunted growth, digestive diseases, and poor carcass quality [4-6]. Although the etiology of IUGR derives from maternal, fetal, placental, or genetic causes, accumulating evidence in humans and experimental animals demonstrated that the majority of IUGR cases principally point to a failure of the placenta associated with a decrease in maternal-fetal nutrients and oxygen exchange [1, 7, 8]. However, the pathophysiological mechanisms underlying placental dysfunction-induced IUGR in pigs remain poorly understood.

The placenta is a transient organ that only persists for the duration of pregnancy but is absolutely crucial for all intrauterine events [9], fulfilling key tasks to transporting nourishment, producing hormones and cytokines, acting as a waste filtration system, and as a protective barrier to guarantee physiological adaptations of mother and fetus during pregnancy [10, 11]. Porcine placenta belongs to epitheliochorial type, where columnar trophoblasts lack significant invasion but spread loosely over the uterine luminal epithelial layer to form the folded bilayer [12]. Previous studies have indicated that the reduction in utero-placental blood flows and/or angiogenesis contribute to insufficient transport of nutrients and fetal hypoxia that is likely to be related to formation of IUGR fetuses [8, 13]. Interactions between placental trophoblast cells and maternal immune cells are also known to have an influence on the growth trajectories of a fetus [9]. Proteomics analysis revealed that the placenta and endometrium of IUGR pig fetuses are vulnerable to nutrient transport reduction, oxidative damage, and impairment of cell

metabolism [14]. Placental structure is also an important factor in determining placental efficiency. Previous studies showed that the placental folds (PFs), especially the shape of trophoblast cells, and the expression of regulatory genes of Meishan pigs underwent more complex changes than those of Yorkshire pigs, and such changes may be a potential factor for their differences in reproductive performance.

The placenta possess a unique transcriptional landscape throughout pregnancy, so its growth and development are regulated by sophisticated pathways composed of the expression of substantial genes [11, 15]. Incorrect alterations in gene expression in placenta give rise to abnormal morphologies and dysfunction have been found to be associated with various pregnancy complications [11, 16]. The development of pig placenta reaches completion in terms of weight, surface area, and numbers of placental areolae by days 60–70 of gestation [17], which is crucial for fetal growth and development in late gestation. However, transcriptome analysis of placenta related with pig IUGR fetuses in this period is rarely reported. The present study aimed to identify the differentially expressed genes (DEGs) in the placentas of fetuses with lightest weight (LW) compared with those in the placentas of mean-weight (MW) litter during day 65 (D65) of gestation through mRNA sequencing, and illustrate the function of RACK1 on porcine trophoblast cells. The findings could provide basic reference for future etiological mechanisms of IUGR in pigs.

2 Materials and Methods

2.1 Ethics statement

All experimental design and protocols in this study were reviewed and approved by the Institutional Animal Care and Use Committee of Guizhou University, Guiyang, China (EAE-

GZU-2020-T010). All efforts were made to minimize animal suffering.

2.2 Tissue collection

Five Duroc sows showing signs of spontaneous estrus and with similar litter size record, parity, and weight were artificially inseminated twice daily with the semen from the same Duroc boar. All sows were raised under similar conditions. After the pregnant sows were hysterectomized after the induction of anesthesia (xylazine, 2.0 mg/kg bw) during D65 of pregnancy, the uteri were opened from the corners. At the time of dissection, all fetuses were identified as "live" or "dead," and their sex was determined on the basis of their morphology. Each fetus was weighed, and the corresponding placenta sample was collected and immediately snap-frozen in liquid nitrogen and stored at −80 °C. The LW fetuses and those closest to the MW of the litter were identified and chosen on the basis of fetal body weights. Meanwhile, the placenta samples were fixed in 4% paraformaldehyde used for histomorphological examination.

2.3 Histomorphological analysis

The placental tissues were fixed in 4% paraformaldehyde for a minimum of 48 h and then embedded in paraffin, sectioned with 5 μm thickness, and stained with hematoxylin–eosin (H&E) on the basis of standard histological criteria. Subsequently, placental histomorphometry of the stained sections was executed as described previously [18, 19]. Placental data were obtained using a Nikon Ni-U light microscope (100× magnification) fitted with a Nikon (DS-Fi1) digital camera (Nikon, Japan). Morphometric measurements of the average width of the PFs and fold length (μm) per micrometer of placenta were calculated using ImageJ 1.45 software (National Institutes of Health, Bethesda, MD).

2.4 Total RNA isolation and RNA sequencing

Eight placenta samples of the fetus with LW (male, n = 4) and closest to the MW (male, n = 4) of the litter were selected for RNA sequencing. The total RNA was extracted from the placental tissues with the Total RNA Kit (Omega, USA) in accordance with the manufacturer's instructions. The RNA quality and amounts were evaluated using a 2100 Bioanalyzer (Agilent Technologies, Santa Clara, CA) and agarose gel electrophoresis. All extractions exhibiting an RNA integrity number > 7.0 and a 28S:18S ratio > 1.0 were used in the next experiments. mRNA sequencing was carried out on the Illumina Hiseq 2500 system (Illumina, San Diego, CA, USA) and 150 bp paired-end FASTQ read files were generated. Raw data were deposited in the NCBI Sequence Read Archive database under accession number PRJNA838349. They were filtrated to obtain clean reads by removing adaptor and low-quality reads. The clean reads were aligned with the Ensembl *Sus scrofa* reference genome (version:scrofa10.2.87) by using Hisat2 version 2.0.5 [20], followed by transcript assembly and differential transcript expression analysis with Cufflinks version 2.2.1. Gene expression was measured with fragments per kilobase million mapped reads (FPKM) by using Cufflinks version 2.2.1. DESeq2 was used to normalize the read counts and apply FPKM values to calculate the relative gene expression differences by adjusting *P* values via Benjamini and Hochberg's method to control the false discovery rate (FDR) and fold change (FC). Differentially expressed genes (DEGs) were screened out when the adjusted p-value < 0.05 and $|\log_2 FC| \geq 1$. Gene ontology (GO) annotation and Kyoto Encyclopedia of Genes and Genomes (KEGG) pathway analysis were performed on all DEGs by using KOBAS 3.0 (http://kobas.cbi.pku.edu.cn), and the DEGs were considered significant at FDR < 0.05.

2.5 Construction of protein–protein interaction (PPI) network

The Search Tool for the Retrieval of Interacting Genes (STRING) database (https://string-db.org/) is utilized to identify the pairwise relationships of all DEGs by computational prediction methods. In this study, STRING was used to predict the interactions among proteins encoded by candidate genes, with cutoff for confidence scores of interactions > 0.4. Cytoscape software (https://cytoscape.org/) was applied to visualize the results of the PPI network. Molecular Complex Detection (MCODE), a Cytoscape plugin, was used to locate the hub genes of the PPI network with the number of nodes > 10.

2.6 Quantitative real-time PCR (qRT-PCR)

cDNA was generated from 1 μg of total RNA by using the PrimeScript RT Reagent Kit (Takara, Japan) in accordance with the manufacturer's protocol as previously described [21]. Quantitative PCR was performed on QuantStudio 3 (Applied Biosystems, MA, USA) following the parameters recommended by the manufacturer. Each reaction mixture (10 μL) contained 1 μL of cDNA solution, 0.3 μL of 10 mM of each specific primer, 5 μL of SYBR Select Master Mix, and 3.4 μL of ddH_2O. The PCR reactions were run as follows: initial denaturation at 95 °C for 2 min; 40 cycles of denaturation at 95 °C for 15 s; annealing at 60 °C for 15 s, with an extension at 72 °C for 1 min; and finally, a melting curve was drawn at 95 °C for 15 s, 60 °C for 1 min, and 95 °C for 15 s. **Table 1** shows the primer information of target genes. Each gene expression test was performed in triplicates. The specificity of the PCR reaction was confirmed through a single peak in the melting curve. Gene expression levels were normalized with β-actin to calculate the relative expression levels by using the $2^{-\Delta\Delta Ct}$ method.

155 **Table 1. Primers used for qPCR.**

Genes	Primer Sequences (5′–3′)	Product Size (bp)	GenBank Accession No.
RACK1	F: GCTGACCAGAGATGAGACCAAT R: TCGGGAGCCAGAGACAATTTG	244	NM_214332
RPL13	F: CAGCAGGAATGGCATGAT R: ATCCACCGAGATCCCAAT	289	NM_001243345
RPL3	F: GGCAGGATGAGATGATTGATGT R: TCTCTGTGCGGTGATGGTAG	204	NM_001244063
RPL35	F: ACTGGAGGACCTGAAGGTGGAG R: CTTCCGCTGCTGCTTCTTGGT	271	NM_214326
RPS3	F: CGAGGTCGTGGTGTCTGGGAAA R: GTGGTCAGGCAGCGGCTTCTTA	220	NM_001044601
RPSA	F: GCCGCTTCACTCCTGGAACCTT R: GGCGAGCATCCACCACATCAGA	236	NM_001037146
β-Actin	F:CCACGAGACCACCTTCAACTC R:TGATCTCCTTCTGCATCCTGT	131	DQ845171

156 ## 2.7 Construction of RACK1 overexpression plasmid

157 The coding sequences (CDS) of the porcine RACK1 gene were amplified from the NCBI
158 database (https://www.ncbi.nlm.nih.gov/nuccore/NM_214332.1). The RACK1 CDS was
159 analyzed to identify appropriate restriction enzymes for vector construction using Primer 5.0
160 software (PRIMER-E Ltd., Plymouth, UK). The recombinant plasmid containing the RACK1
161 CDS and the pEGFP-C1 plasmid were subjected to digestion with *Sal*I and *Xba*I, and the linked
162 product was subsequently used to transform competent DH5α. Endotoxin-free plasmids
163 containing the correct fragment were identified by restriction enzyme digestion and sequencing.

164 ## 2.8 Cell culture and transfection

165 Porcine trophoblast cell line PTr2 were kindly provided from South China Agricultural
166 University as previously described [22]. The PTr2 cells were cultured in DMEM-F12 (Gibco,

Waltham, MA, USA) supplemented with 10% fetal bovine serum (Gibco, Carlsbad, CA, USA) and recombinant human insulin (Yeasen, Shanghai, China) and maintained at 37 °C with 5% CO_2 humidified atmosphere. They were then transferred into a six-well plate with 0.25–1 × 10^6 cells per well and transfected with pEGFP-C1- RACK1 and pEGFP-C1 plasmid by Lipo8000 (Beyotime, Shanghai, China) in accordance with the manufacturer's protocol.

2.9 Cell proliferation and migration assay

The cell proliferation in this study was assessed by cell counting kit-8 (CCK8) assay (Solarbio, Beijing, China). The PTr2 cells were seeded on 96-well plates with 100 μL of complete culture medium; treated with pEGFP-C1- RACK1, and pEGFP-C1 plasmid; and incubated for increasing durations (0, 12, 24, and 48 h). Then, 10 μL of the CCK8 solution was added per well and incubated for 2 h at 37 °C. Absorbance was measured at 450 nm with a microplate reader (CYTATION5, BioTek, USA).

Wound healing assay was performed to analyze the influence of overexpressed RACK1 on PTr cell migration as described elsewhere. In brief, 2 × 10^5 cells were inoculated in F12 medium containing 10% FBS and 0.1% insulin. After the cells reached 80–90 % confluence, a perpendicular wound was established by creating a linear cell-free region with the use of a 10 μL pipette tip. The cells were washed with PBS twice, fresh complete medium was added, and the overexpressed vector and empty vector were transfected into the cells at the same time. The progress of cell migration into the scratch was photographed at 0 and 24 h after wounding with the use of computer-assisted microscopy. The images were quantitatively analyzed using ImageJ software (National Institutes of Health, Bethesda, MD). Cell migration was calculated as percentages of cell coverage to the initial cell-free zone.

2.10 Statistical analysis

The placental histomorphological data and mRNA expression levels were analyzed via one-way analysis of variance using SPSS 19.0 software (IBM Corp., Armonk, NY, USA). The data for the CCK8 and wound healing assays were evaluated using Student's t-Test. All data are presented as mean ± standard error of mean (SEM). $P < 0.05$ was considered statistically significant.

3 Results

3.1 Fetal and placental characteristics in pigs at D65 of pregnancy

In this study, all five sows from artificial insemination were pregnant, and they produced 42 live and three dead fetuses at D65 of pregnancy. The average body weight of pig fetuses was 204.4 g, with a range of 134–259 g (**Fig 1A**). Corresponding maternal–fetal interface samples of fetuses with LW and MW of the litter were collected to investigate the associations of fetal weight and placental morphologies and functions. Next, the histomorphologies of the maternal–fetal interface of the LW and MW fetuses were compared by the sections stained with H&E. The results of observations revealed that the folded structure of the epithelial bilayer of the LW placentas followed a poor and incomplete development compared with that of the MW placentas (**Fig 1B**). The morphometry analysis showed that the fold width and fold length (μm) per micrometer of the LW placentas were extremely significantly lower than those of the MW placentas (**Fig 1C** and **1D**, $P < 0.001$).

Fig 1. **Characteristics of fetal weight and placental morphology in pigs during day 65 of gestation.** (**A**) Distribution of fetal body weight. (**B**) Photomicrographs of representative sections of maternal–fetal interface derived from fetuses with lightest weight (LW) and litter

with mean weight (MW) and stained with hematoxylin and eosin. Placental trophoblast (Tr) that came into touch with endometrial luminal epithelium (LE) to form placental folds (PF). (**C**) Width of PFs and (**D**) fold length (μm) per micrometer of placenta used to compare placental morphometry. PS, placental stroma; $**p < 0.01$; $***p < 0.001$

3.2 Differences in transcriptomic profiles between LW and MW placentas

After trimming for adapters and removing the low-quality reads, RNA-seq libraries that generated 40.6–41.7 million sequence reads among samples were used for downstream analysis. A total of 41,150,783 and 41,396,695 clean reads and 32,991,736 and 33,325,260 mapped reads were obtained from the LW and MW placentas, respectively (**S1 Table**). Through gene expression analysis (q-value < 0.05; FC > 2), 632 genes were identified to be significant DEGs between the LW and MW placentas (**S1 Fig**), and 535 and 119 genes were upregulated and downregulated in the LW placentas, respectively. Hierarchical clustering was performed with the datasets of DEGs. The mRNA expression patterns of the LW and MW placenta samples were clustered separately after clustering (**Fig 2**).

Fig 2. Heatmap of differentially expressed genes (DEGs) in LW and MW placentas. Orange and green represent genes with high and low expression levels, respectively.

3.3 GO function and KEGG pathway analysis of DEGs

GO enrichment analysis revealed that the DEGs mainly functionally enriched in biological processes were protein ubiquitination; signal transduction by protein phosphorylation; cytoplasmic translation; translational elongation; positive regulation of GTPase activity; positive regulation of transcription by RNA polymerase II; and negative regulation of transcription, DNA-templated (**Fig 3A**). The cellular components were mainly composed of

polysomal ribosome, nucleus, cytosol, cytoplasm, and cytosolic large ribosomal subunit (**Fig 3B**). For GO molecular function, ATP binding, DNA binding, protein kinase binding, ribonucleoprotein complex binding, and RNA binding were the most significantly enriched terms. KEGG pathway enrichment analysis showed that the DEGs of the two groups of placentas participated in ribosome pathway, endocytosis, mTOR signaling pathway, phagosome, lysosome, and regulation of actin cytoskeleton.

Fig 3. GO enrichment and KEGG pathway analysis of differentially expressed genes (DEGs) between LW and MW placentas. (**A**) Biological process term of GO enrichment analysis. (**B**) Cellular component term of GO enrichment analysis. (**C**) Molecular function term of GO enrichment analysis. (**D**) KEGG pathway analysis of DEGs. GO: Gene Ontology; KEGG: Kyoto Encyclopedia of Genes and Genomes.

3.4 PPI network and MCODE analysis

A PPI network of the DEGs with 544 nodes and 1263 edges was constructed through STRING analysis to identify the functions of the DEGs (**Fig 4A)**. The MCODE application in Cytoscape software was used to perform gene network clustering analysis to identify the key PPI network modules. The MCODE results with the parameter K-Core = 2 showed that one significant module was screened out from the PPI network (**Fig 4B**). A total of 15 nodes and 206 edges were found, and *RACK1*, *RPL13*, *EEF2*, *RPS3*, *ABCE1*, *EEF1D*, *RPL3*, *RPL10A*, *RPL35*, *RPLP1*, *RPL12*, *RPL18*, *RPL27A*, *EEF1G*, and *RPSA* were hub nodes in the module with score = 14.714 (**Fig 4B**). KEGG pathway analysis demonstrated that most hub genes were involved in the ribosome pathway based on KOBAS database (**Table 2**). Besides, RNA-sequencing results were confirmed by qRT-PCR. The results showed that in the LW placentas,

256 the mRNA expression levels of *RACK1*, *RPL13*, *RPS3*, *RPL3*, and *RPL35* were significantly
257 lower ($p < 0.05$) and *RPSA* did not differ ($p > 0.05$) compared with those in MW placentas (**Fig**
258 **5**). Increasing evidence have shown that RACK1 had roles on and off the ribosome (23, 24),
259 suggesting that RACK1 may affect the growth and development of trophoblast cells via
260 regulating ribosome function.

261 **Fig 4. Protein–protein interaction (PPI) network and MCODE analysis.** (**A**) PPI network
262 constructed by STRING. The size of each node is positively correlated to the number of degrees.
263 Interactions are shown by edges, with thicker edges corresponding to stronger associations. (**B**)
264 MCODE analysis of differentially expressed genes. The red round nodes represent upregulated
265 genes; the green square nodes represent downregulated genes.

266 **Table 2. List of differentially expressed genes in a significant MCODE module from PPI**
267 **network.**

Accession	Gene Name	FC (LW/MW)	*q*-value	Pathway
ENSSSCG00000024974	RPL13	0.464	0.00417	Ribosome
ENSSSCG00000014855	RPS3	0.401	0.00821	Ribosome
ENSSSCG00000000089	RPL3	0.487	0.02902	Ribosome
ENSSSCG00000001543	RPL10A	0.490	0.03409	Ribosome
ENSSSCG00000005595	RPL35	0.429	0.04763	Ribosome
ENSSSCG00000004970	RPLP1	0.393	0.01018	Ribosome
ENSSSCG00000005612	RPL12	0.447	0.03043	Ribosome
ENSSSCG00000022059	RPL27A	0.404	0.00234	Ribosome
ENSSSCG00000011266	RPSA	0.324	0.00604	Ribosome
ENSSSCG00000025928	RPL18	0.445	0.01216	/
ENSSSCG00000029724	RACK1	0.491	0.03610	Measles

ENSSSCG00000025675	EEF2	0.442	0.03473	AMPK signaling pathway/Oxytocin signaling pathway
ENSSSCG00000006954	EEF1D	0.437	0.04000	/
ENSSSCG00000013064	EEF1G	0.394	0.00018	Legionellosis
ENSSSCG00000009043	ABCE1	2.415	0.01964	/

/ denotes that the gene was not enriched into any KEGG pathway; FC: fold change.

Fig 5. Validation of differentially expressed genes between LW and MW placentas by q-PCR. Values are presented as mean ± SEM. Values labeled with asterisk (*) indicate they are significantly different ($p < 0.05$).

3.5 Promotion of the proliferation and migration of PTr2 cells by RACK1 overexpression

RACK1 was overexpressed in PTr2 cells by transfection with pEGFP-C1-RACK1 plasmid to further explore whether it was involved in the biological behavior of trophoblast cells in this experiment (**S2 Fig**). The CCK8 assay revealed that overexpression of RACK1 significantly increased the proliferation of PTr2 cells compared to the corresponding negative control (**Fig 6**). Wound healing assays were also conducted To further confirm the role of RACK1 in trophoblast migration. The results demonstrated that overexpression of RACK1 increased the migratory ability of PTr2 cells compared with the corresponding negative control (**Fig 7**). These results suggested that RACK1 is required in the migration and proliferation of porcine trophoblasts.

Fig 6. **Effects of RACK1 overexpression on proliferation of PTr2 cells.** (**A**) Microscopic results of PTr2 cells transfected with pEGFP-C1-RACK1 plasmid vector (vector-RACK1) and corresponding negative control vector (vector-NC) after 24 and 48 h. (**B**) Time-dependent cell

viability of PTr2 cells with stable RACK1 overexpression measured by CCK-8 assay, which was evaluated using Student's *t*-test. CCK8, Cell Counting Kit-8. Data are shown as mean ± SEM. ***$P < 0.001$.

Fig 7. Effects of RACK1 overexpression on migration of PTr2 cells. (**A**) Representative wound healing photomicrographs and (**B**) quantitative analysis of wound healing rates of PTr2 cells with stable RACK1 overexpression transfection after 0 and 24 h. These tests were repeated three times independently. The wound healing assay was evaluated using Student's *t*-test. Data are presented as mean ± SEM. ***$P < 0.001$.

4 Discussion

Numerous studies during the past decades have confirmed that placental insufficiency is responsible for the abnormal growth trajectory of a fetus [25, 26]. Improved understanding of the mechanisms governing fetal growth is conducive to reduce the prevalence of low birthweight in pig production industry. Placental structure is compactly associated with its function and fetal growth and development. The results of the present study showed that low-weight pig fetuses had poor and incomplete PFs. In the epitheliochorial placenta, PFs could increase the contact area between trophoderm and endometrial epithelium to ensure that the fetus receives adequate nutrition from the maternal circulation. This finding was consistent with several previous findings that significant differences in placental microscopic folds between large and small pig fetuses due to the development of PFs have a substantial effect on placental efficiency [19, 27].

The development of PFs is associated with facilitating placental efficiency, so the efficiency of nutrient transport from the pregnant sow to the developing fetus depends on the

size and function of the placenta [19]. Therefore, poor placental development may contribute to compromised nutrient transport that gives rise to low fetal body weight. The epitheliochorial placenta initially appears around days 26–30 of gestation, and regular PFs are formed on day 50 of gestation in pigs [22,28,29]. Recent findings in pigs revealed that large fetuses had higher trophoblastic epithelium of the chorioallantois fold than small fetuses at days 45 and 60 of gestation [30]. However, the width of the folded bilayer in the placentas of small fetuses was greater than that in the placentas of large fetuses on day 105 of gestation because PFs underwent rapid increase from mid- to late pregnancy that serves as a compensation in morphometric changes to increasing the surface area of interaction and then improving placental efficiency in response to low fetal weight and reduced placental size [13, 19].

RNA sequencing showed the differences in gene expression pattern between the LW and MW placentas and the multiple genes involved in the ribosomal pathway and mTOR signaling pathway in the LW placentas. Any disturbance in the ribosome environment could have devastating effects on placental development [31, 32]. Ribosomal proteins (RPs) are essential in regulating translation for facilitating placental growth and development [33]. Previous studies have found that many genes encoding ribosomal proteins were in the IUGR placenta [34]. mTOR signaling pathway have been reported to participate in the regulation of cellular activities of trophoblast in multiple pregnancy complications, including IUGR [35]. In human IUGR placenta, the downregulation of the expression of ribosomal proteins (RPL26 and RPS10) was regulated by the mTORC1 signaling pathway, affecting protein synthesis and leads to placental dysfunction [36]. Several reports have indicated that decreased protein synthesis and/or increased protein degradation is a constant feature during fetal growth restriction [37-

39]. Hence, dysregulated expression of RP genes may alter the morphologies of LW placenta via affecting the translation and protein synthesis of trophoblast cells.

Through transcriptomic analysis and in-vitro experiment, this study further found that RACK1 potentially plays a critical role in placental development by regulating the proliferation and migration of porcine trophoblast cells. The migration of trophoblasts at the maternal-fetal interface after implantation is a critical process in placentation to facilitate the establishment of feto-placental circulation and thus essential for successful pregnancy outcomes in mammals [40]. Accumulating evidence has shown that RACK1 is involved in diverse biological processes, including protein translation, cell growth, cell cycle progression, cell migration, and stress responses, by localizing to different subcellular structures, including the nucleus, ribosome, and midbody [41-44]. This finding is consistent with the results of enrichment analysis of DEGs between the MW and LW placentas in the present study. Furthermore, studies on model animals have confirmed that knockdown of RACK1 suppresses cell growth in cultured cells and homozygous knockout of RACK1 is lethal for the embryo [45-47]. A recent study on pigs has shown that the proliferation and invasion of trophoblast cells affect the formation and development of PFs [27]. Therefore, the downregulation of RACK1 in the LW placentas may lead to abnormal development of PFs through inhibiting the proliferation and migration of porcine trophoblast cells, which possibly is a potential cause of fetal growth restriction.

In conclusion, this study demonstrated that the folded structure of the epithelial bilayer of placentas supplying LW fetuses followed a poor and incomplete development compared with that of the placentas supplying MW fetuses at D65 of gestation. A total of 632 DEGs were

352 screened out between the LW and MW placentas, and they were mainly enriched in translation,
353 ribosome, protein synthesis, and mTOR signaling pathway. The data also revealed that RACK1
354 was downregulated in the LW placenta. The decreased RACK1 in the LW placentas may be
355 involved in the abnormal development of PFs by inhibiting the proliferation and migration of
356 porcine trophoblast cells. Further works are required to elucidate the detailed molecular
357 mechanisms underlying RACK1 in the regulation of porcine trophoblast cells.

358 Conflicts of Interest

359 The authors declare that there is no conflict of interest that could be perceived as
360 prejudicing the impartiality of the research reported.

361 Declaration of Funding

362 This study was supported by two grants received from the Department of Science and
363 Technology of Guizhou Province, China (No. QKHJC-ZK[2021]YB166 and No.
364 QKHZC[2021]YB147), the China Scholarship Council (No. LJM [2021]109) the Youth
365 Science and Technology talent Development Project of Education Department of Guizhou
366 Province, China (No. QJHKYZ[2021]081), the Guizhou Outstanding Young Scientific and
367 technological Talents Training Program (No. QKHPTRC[2021]5630), the Scientific Research
368 Project of Guizhou University Talents Fund (No. GDRJHZ-2019-21) and the Guizhou Pig
369 Industry Development Project (2021).

370 Author contributions

371 Zheng Ao and Zhimin Wu conceived and designed the study; Guangling Hu and Zhimin Wu
372 and Ting Gong acquired the data; Zheng Ao, Zhimin Wu and Yiyu Zhang analyzed and
373 interpreted the data; Qun Hu and Linjun Hong contributed to contributed materials; Zheng Ao
374 and Zhimin Wu wrote and revised the paper.

References

1. Thorn SR, Rozance PJ, Brown LD, Hay WW, editors. The intrauterine growth restriction phenotype: fetal adaptations and potential implications for later life insulin resistance and diabetes. Seminars in Reproductive Medicine; 2011;29:225-236
2. Armengaud J, Yzydorczyk C, Siddeek B, Peyter A, Simeoni U. Intrauterine growth restriction: Clinical consequences on health and disease at adulthood. Reproductive Toxicology. 2021;99:168-176.
3. Wu G, Bazer F, Burghardt R, Johnson G, Kim S, Li X, et al. Impacts of amino acid nutrition on pregnancy outcome in pigs: mechanisms and implications for swine production. Journal of Animal Science. 2010;88(suppl_13):E195-E204.
4. D'Inca R, Kloareg M, Gras-Le Guen C, Le Huërou-Luron I. Intrauterine growth restriction modifies the developmental pattern of intestinal structure, transcriptomic profile, and bacterial colonization in neonatal pigs. The Journal of Nutrition. 2010;140(5):925-931.
5. Wu G, Bazer F, Wallace J, Spencer T. Board-invited review: intrauterine growth retardation: implications for the animal sciences. Journal of Animal Science. 2006;84(9):2316-37.
6. Gao H, Zhang L, Wang L, Liu X, Hou X, Zhao F, et al. Liver transcriptome profiling and functional analysis of intrauterine growth restriction (IUGR) piglets reveals a genetic correction and sexual-dimorphic gene expression during postnatal development. BMC Genomics. 2020;21(1):1-16.
7. Balayla J, Desilets J, Shrem G. Placenta previa and the risk of intrauterine growth restriction (IUGR): a systematic review and meta-analysis. Journal of Perinatal Medicine. 2019;47(6):577-584.
8. Chassen S, Jansson T. Complex, coordinated and highly regulated changes in placental signaling and nutrient transport capacity in IUGR. Biochimica et Biophysica Acta (BBA)-Molecular Basis of Disease. 2020;1866(2):165373.
9. Woods L, Perez-Garcia V, Hemberger MJFie. Regulation of placental development and its impact on fetal growth—new insights from mouse models. Frontiers in Endocrinology. 2018;9:570.
10. Medina-Bastidas D, Guzman-Huerta M, Borboa-Olivares H, Ruiz-Cruz C, Parra-Hernandez S, Flores-Pliego A, et al. Placental Microarray Profiling Reveals Common mRNA and lncRNA Expression Patterns in Preeclampsia and Intrauterine Growth Restriction. International Journal of Molecular Sciences. 2020;21(10):3597.
11. Majewska M, Lipka A, Paukszto L, Jastrzebski JP, Szeszko K, Gowkielewicz M, et al. Placenta transcriptome profiling in intrauterine growth restriction (IUGR). International Journal of Molecular Sciences. 2019;20(6):1510.
12. Furukawa S, Kuroda Y, Sugiyama AJJotp. A comparison of the histological structure of the placenta in experimental animals. Journal of Toxicologic Pathology. 2014;27(1):11-18.
13. Wang J, Feng C, Liu T, Shi M, Wu G, Bazer FWJMR, et al. Physiological alterations associated with intrauterine growth restriction in fetal pigs: causes and insights for nutritional optimization. Molecular Reproduction and Development. 2017;84(9):897-904.
14. Chen F, Wang T, Feng C, Lin G, Zhu Y, Wu G, et al. Proteome differences in placenta and endometrium between normal and intrauterine growth restricted pig fetuses. PLoS One. 2015;10(11):e0142396.
15. Majewska M, Lipka A, Paukszto L, Jastrzebski JP, Gowkielewicz M, Jozwik M, et al. Preliminary RNA-seq analysis of long non-coding RNAs expressed in human term placenta. International Journal of Molecular Sciences. 2018;19(7):1894.
16. Li N, Hou R, Liu C, Yang T, Qiao C, Wei JJCp. Integration of transcriptome and proteome profiles in placenta accreta reveals trophoblast over-migration as the underlying pathogenesis. Clinical Proteomics. 2021;18(1):1-

12.
17. Bazer FW, Johnson GA. Pig blastocyst–uterine interactions. Differentiation. 2014;87(1-2):52-65.
18. Ao Z, Li Z, Wang X, Zhao C, Gan Y, Wu X, et al. Identification of amniotic fluid metabolomic and placental transcriptomic changes associated with abnormal development of cloned pig fetuses. Molecular Reproduction and Development. 2019;86(3):278-291.
19. Vallet J, Freking B. Differences in placental structure during gestation associated with large and small pig fetuses. Journal of Animal Science. 2007;85(12):3267-75.
20. Pertea M, Kim D, Pertea GM, Leek JT, Salzberg SL. Transcript-level expression analysis of RNA-seq experiments with HISAT, StringTie and Ballgown. Nature Protocols. 2016;11(9):1650-1667.
21. Ao Z, Liu DW, Zhao CF, Yue ZM, Shi JS, Zhou R, et al. Birth weight, umbilical and placental traits in relation to neonatal loss in cloned pigs. Placenta. 2017;57:94-101.
22. Hong L, He Y, Tan C, Wu Z, Yu M. HAI-1 regulates placental folds development by influencing trophoblast cell proliferation and invasion in pigs. Gene. 2020;749:144721.
23. Johnson AG, Lapointe CP, Wang J, Corsepius NC, Choi J, Fuchs G, et al. RACK1 on and off the ribosome. Rna. 2019;25(7):881-895.
24. Nilsson J, Sengupta J, Frank J, Nissen P. Regulation of eukaryotic translation by the RACK1 protein: a platform for signalling molecules on the ribosome. EMBO Reports. 2004;5(12):1137-41.
25. Krishna U, Bhalerao S. Placental insufficiency and fetal growth restriction. The Journal of Obstetrics and Gynecology of India. 2011;61(5):505-511.
26. Davenport BN, Wilson RL, Jones HN. Interventions for placental insufficiency and fetal growth restriction. Placenta. 2022;125;4-9.
27. Stenhouse C, Hogg CO, Ashworth CJ. Associations between fetal size, sex and placental angiogenesis in the pig. Biology of Reproduction. 2019;100(1):239-252.
28. Hong L, Hou C, Li X, Li C, Zhao S, Yu M. Expression of heparanase is associated with breed-specific morphological characters of placental folded bilayer between Yorkshire and Meishan pigs. Biology of Reproduction. 2014;90(3):56, 1-9.
29. Geisert R, Schmitt R. Early embryonic survival in the pig: can it be improved? Journal of Animal Science. 2002;80(E-suppl_1):E54-E65.
30. Almeida F, Dias AA. Pregnancy in pigs: the journey of an early life. Domestic Animal Endocrinology. 2022;78:106656.
31. Janssen BG, Byun H-M, Gyselaers W, Lefebvre W, Baccarelli AA, Nawrot TS. Placental mitochondrial methylation and exposure to airborne particulate matter in the early life environment: an ENVIR ON AGE birth cohort study. Epigenetics. 2015;10(6):536-544.
32. Reid DS, Burnett DD, Contreras-Correa ZE, Lemley CO. Differences in bovine placentome blood vessel density and transcriptomics in a mid to late-gestating maternal nutrient restriction model. Placenta. 2022;117:122-130.
33. Kondrashov N, Pusic A, Stumpf CR, Shimizu K, Hsieh AC, Xue S, et al. Ribosome-mediated specificity in Hox mRNA translation and vertebrate tissue patterning. Cell. 2011;145(3):383-397.
34. Sitras V, Paulssen R, Leirvik J, Vårtun Å, Acharya G. Placental gene expression profile in intrauterine growth restriction due to placental insufficiency. Reproductive Sciences. 2009;16(7):701-711.
35. Tsai K, Tullis B, Jensen T, Graff T, Reynolds P, Arroyo J. Differential expression of mTOR related molecules in the placenta from gestational diabetes mellitus (GDM), intrauterine growth restriction (IUGR) and preeclampsia patients. Reproductive Biology. 2021;21(2):100503.
36. Rosario FJ, Powell TL, Gupta MB, Cox L, Jansson T. mTORC1 transcriptional regulation of ribosome

subunits, protein synthesis, and molecular transport in primary human trophoblast cells. Frontiers in Cell and Developmental Biology. 2020;8:583801.

37. Regnault T, Friedman J, Wilkening R, Anthony R, Hay Jr W. Fetoplacental transport and utilization of amino acids in IUGR—a review. Placenta. 2005;26:S52-S62.
38. Hay Jr WW. Recent observations on the regulation of fetal metabolism by glucose. The Journal of physiology. 2006;572(1):17-24.
39. Burton GJ, Jauniaux E, Charnock-Jones DS. The influence of the intrauterine environment on human placental development. International Journal of Developmental Biology. 2009;54(2-3):303-311.
40. Silva JF, Serakides R. Intrauterine trophoblast migration: A comparative view of humans and rodents. Cell Adhesion & Migration. 2016;10(1-2):88-110.
41. Adams DR, Ron D, Kiely PA. RACK1, A multifaceted scaffolding protein: Structure and function. Cell Communication and Signaling. 2011;9(1):1-24.
42. Cheng Z-F, Pai RK, Cartwright CA. Rack1 function in intestinal epithelia: regulating crypt cell proliferation and regeneration and promoting differentiation and apoptosis. American Journal of Physiology-Gastrointestinal and Liver Physiology. 2018;314(1):G1-G13.
43. Wang C-C, Lo H-F, Lin S-Y, Chen H. RACK1 (receptor for activated C-kinase 1) interacts with FBW2 (F-box and WD-repeat domain-containing 2) to up-regulate GCM1 (glial cell missing 1) stability and placental cell migration and invasion. Biochemical Journal. 2013;453(2):201-208.
44. Gandin V, Senft D, Topisirovic I, Ronai ZeA. RACK1 function in cell motility and protein synthesis. Genes & Cancer. 2013;4(9-10):369-77.
45. Hu F, Tao Z, Wang M, Li G, Zhang Y, Zhong H, et al. RACK1 promoted the growth and migration of the cancer cells in the progression of esophageal squamous cell carcinoma. Tumor Biology. 2013;34(6):3893-3899.
46. Wang A, Yang W, Li Y, Zhang Y, Zhou J, Zhang R, et al. CPNE1 promotes non-small cell lung cancer progression by interacting with RACK1 via the MET signaling pathway. Cell Communication and Signaling. 2022;20(1):1-16.
47. Yoshino Y, Chiba N. Roles of RACK1 in centrosome regulation and carcinogenesis. Cellular Signalling. 2022;90:110207.

Supporting information

S1 Table. Summary of mapping statistics in LW and MW placenta

S1 Fig. Volcano map of differential expressed genes between LW and MW placentas.

S2 Fig. Transfection efficiency of RACK1 overexpression vector determined by qPCR.

**P < 0.001.

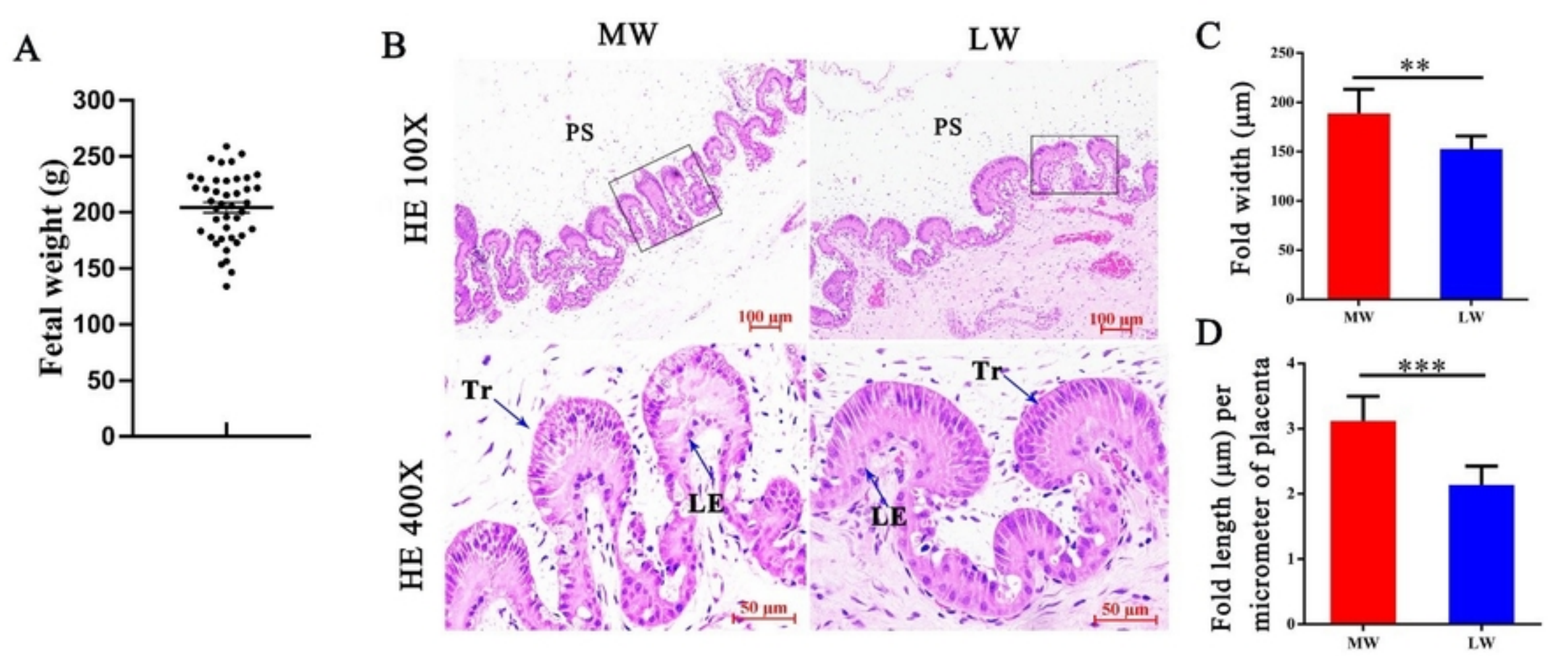
A
Fetal weight (g)
300
250
200
150
100
50
0
B
MW
LW
HE 100X
HE 400X
PS
PS
100 μm
100 μm
Tr
Tr
LE
LE
50 μm
50 μm
C
Fold width (μm)
250
200
150
100
50
0
**
MW
LW
D
Fold length (μm) per micrometer of placenta
4
3
2
1
0
***
MW
LW

Figure

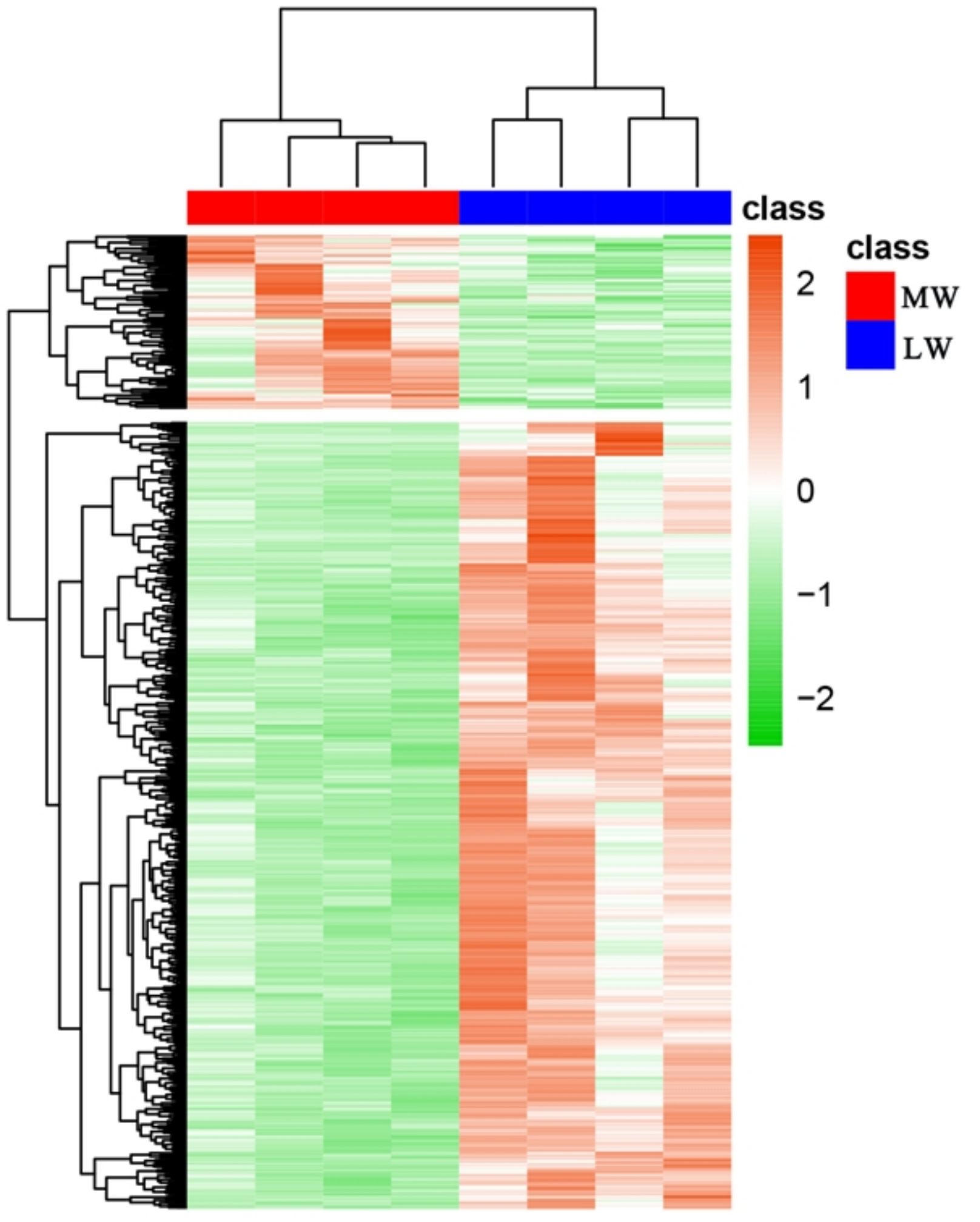

Figure

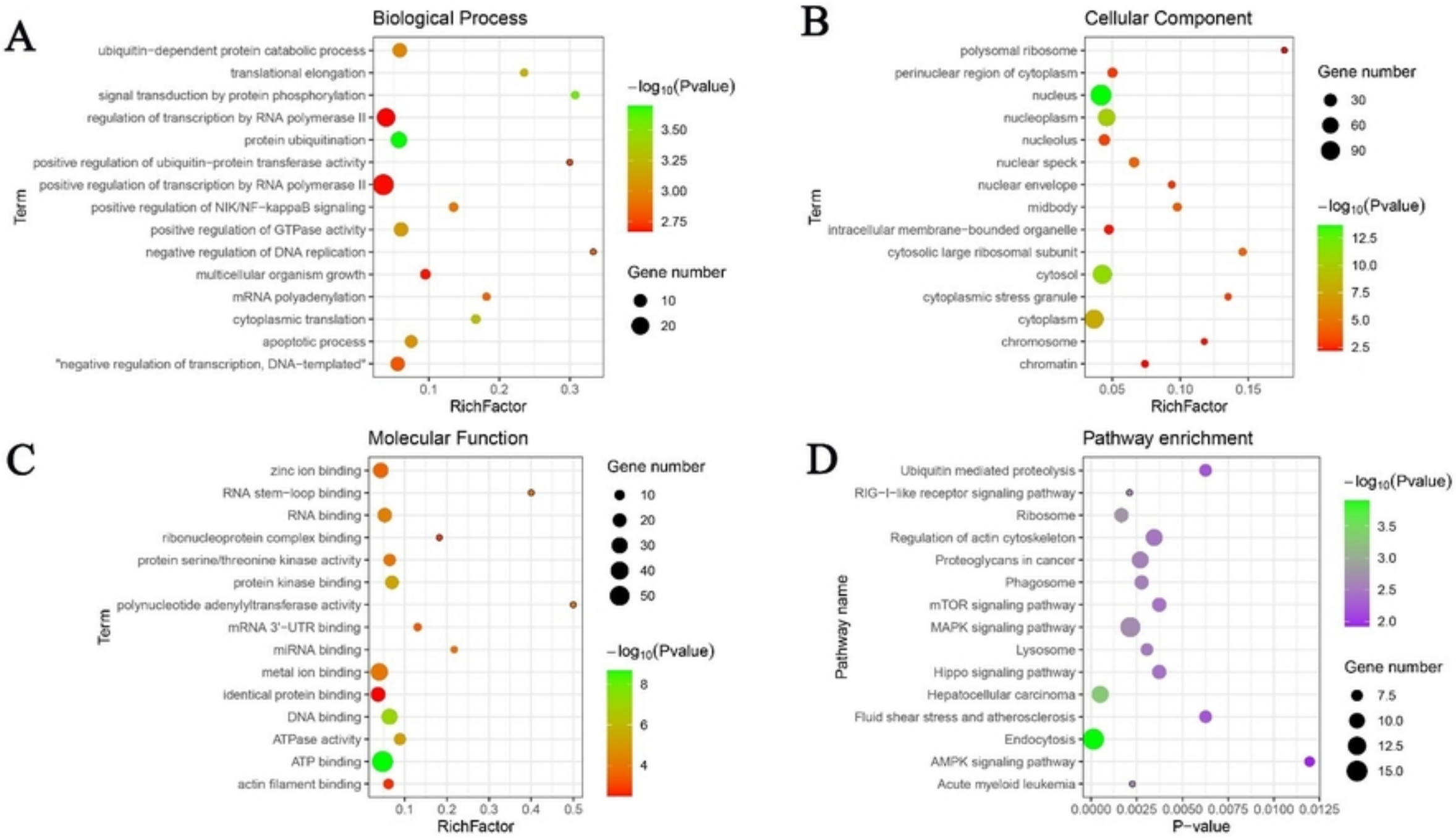
A
Biological Process
ubiquitin−dependent protein catabolic process
translational elongation
signal transduction by protein phosphorylation
regulation of transcription by RNA polymerase II
protein ubiquitination
positive regulation of ubiquitin−protein transferase activity
positive regulation of transcription by RNA polymerase II
positive regulation of NIK/NF−kappaB signaling
positive regulation of GTPase activity
negative regulation of DNA replication
multicellular organism growth
mRNA polyadenylation
cytoplasmic translation
apoptotic process
"negative regulation of transcription, DNA−templated"
Term
0.1
0.2
0.3
RichFactor
−log10(Pvalue)
3.50
3.25
3.00
2.75
Gene number
10
20
B
Cellular Component
polysomal ribosome
perinuclear region of cytoplasm
nucleus
nucleoplasm
nucleolus
nuclear speck
nuclear envelope
midbody
intracellular membrane−bounded organelle
cytosolic large ribosomal subunit
cytosol
cytoplasmic stress granule
cytoplasm
chromosome
chromatin
Term
0.05
0.10
0.15
RichFactor
Gene number
30
60
90
−log10(Pvalue)
12.5
10.0
7.5
5.0
2.5
C
Molecular Function
zinc ion binding
RNA stem−loop binding
RNA binding
ribonucleoprotein complex binding
protein serine/threonine kinase activity
protein kinase binding
polynucleotide adenylyltransferase activity
mRNA 3'−UTR binding
miRNA binding
metal ion binding
identical protein binding
DNA binding
ATPase activity
ATP binding
actin filament binding
Term
0.1
0.2
0.3
0.4
0.5
RichFactor
Gene number
10
20
30
40
50
−log10(Pvalue)
8
6
4
D
Pathway enrichment
Ubiquitin mediated proteolysis
RIG−I−like receptor signaling pathway
Ribosome
Regulation of actin cytoskeleton
Proteoglycans in cancer
Phagosome
mTOR signaling pathway
MAPK signaling pathway
Lysosome
Hippo signaling pathway
Hepatocellular carcinoma
Fluid shear stress and atherosclerosis
Endocytosis
AMPK signaling pathway
Acute myeloid leukemia
Pathway name
0.0000
0.0025
0.0050
0.0075
0.0100
0.0125
P−value
−log10(Pvalue)
3.5
3.0
2.5
2.0
Gene number
7.5
10.0
12.5
15.0

Figure

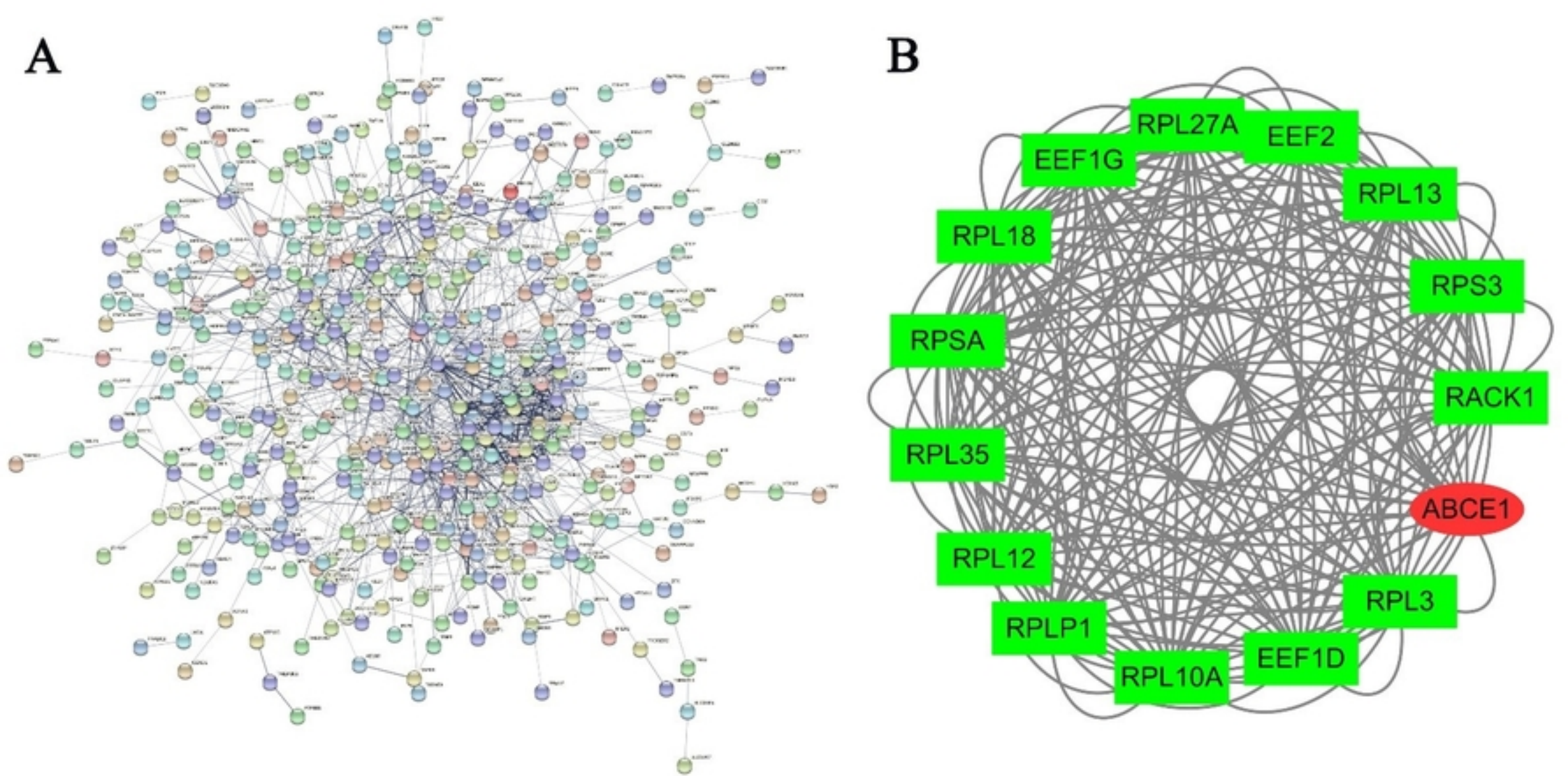
A
B
RPL27A
EEF2
EEF1G
RPL13
RPL18
RPS3
RPSA
RACK1
RPL35
ABCE1
RPL12
RPL3
RPLP1
EEF1D
RPL10A

Figure

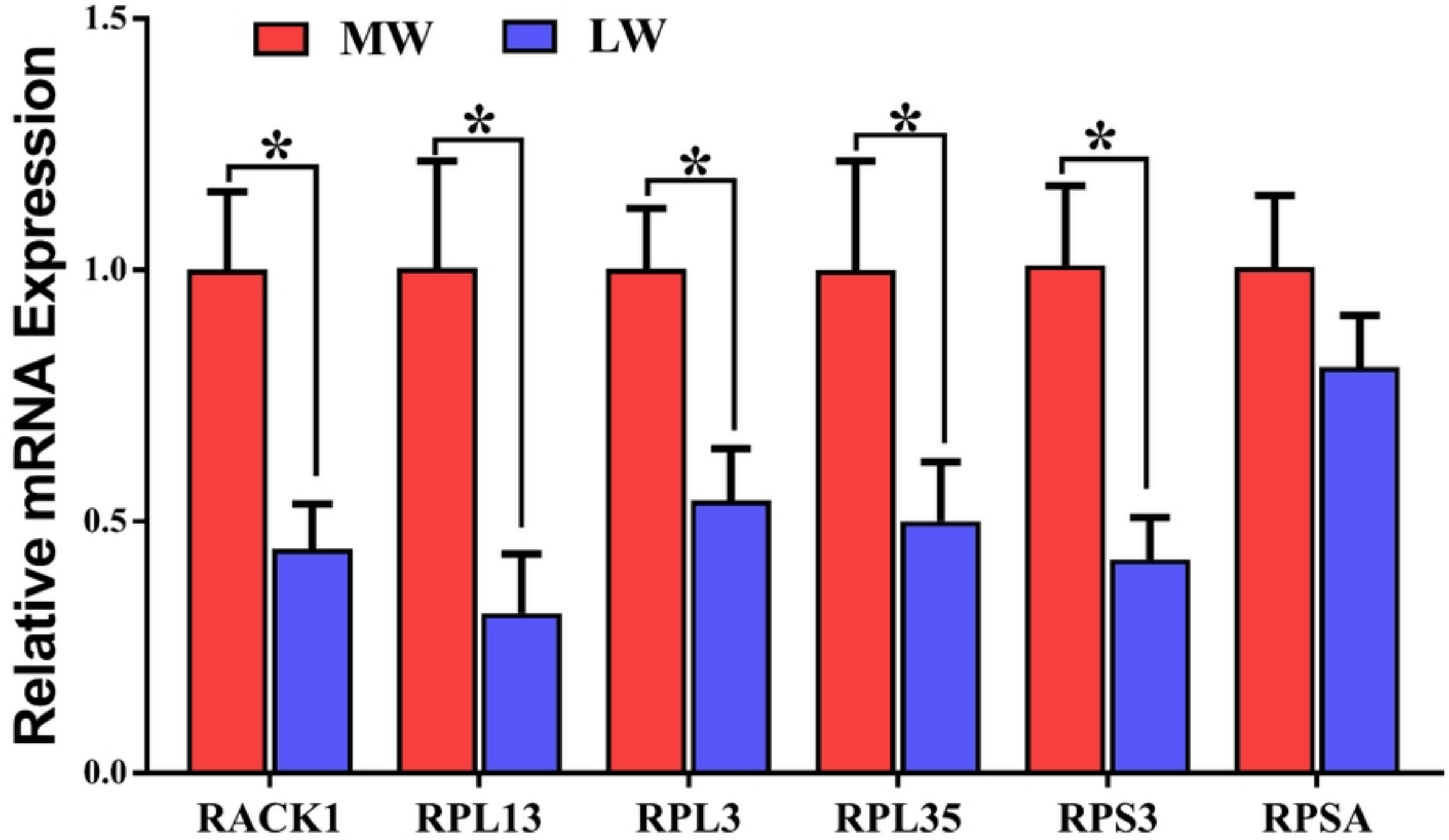
MW
LW
Relative mRNA Expression
1.5
1.0
0.5
0.0
*
*
*
*
*
RACK1
RPL13
RPL3
RPL35
RPS3
RPSA

Figure

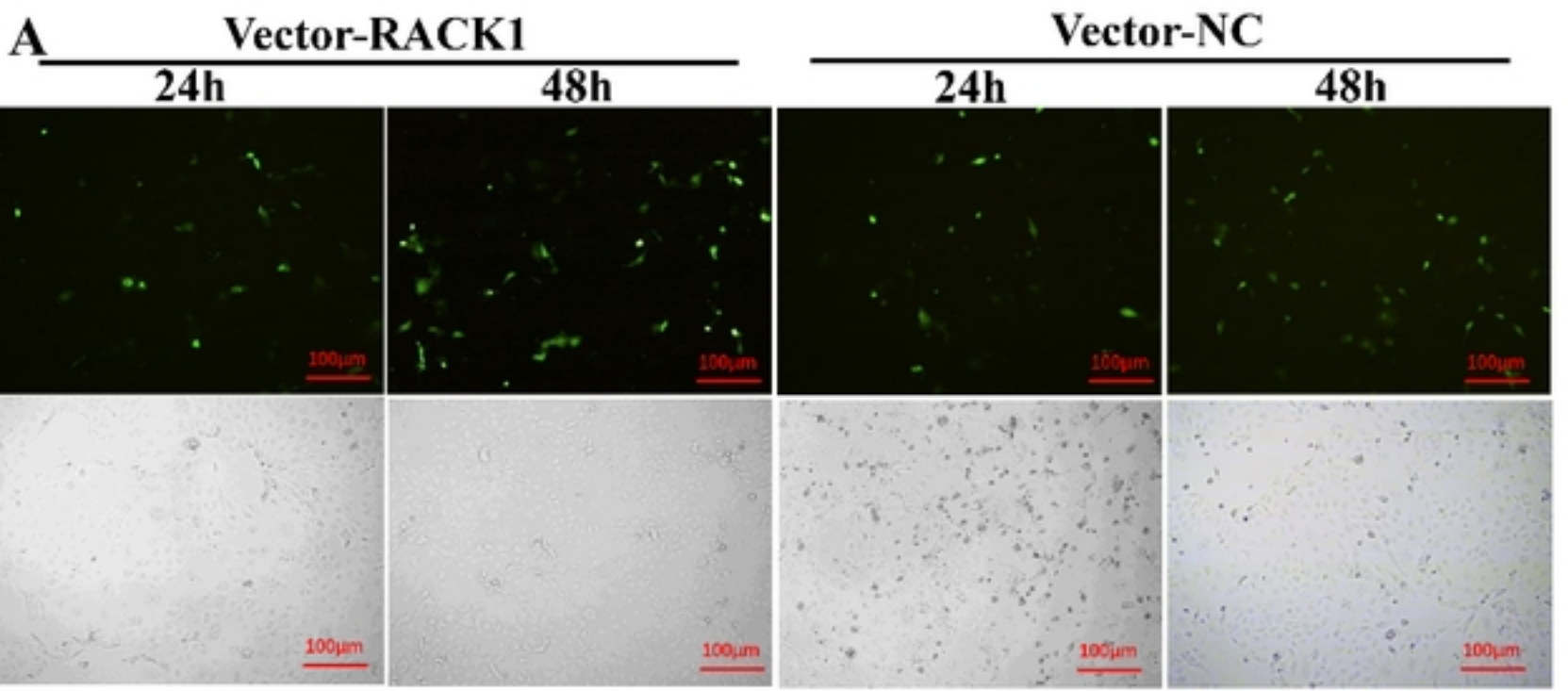
A
Vector-RACK1
Vector-NC
24h
48h
24h
48h
100μm

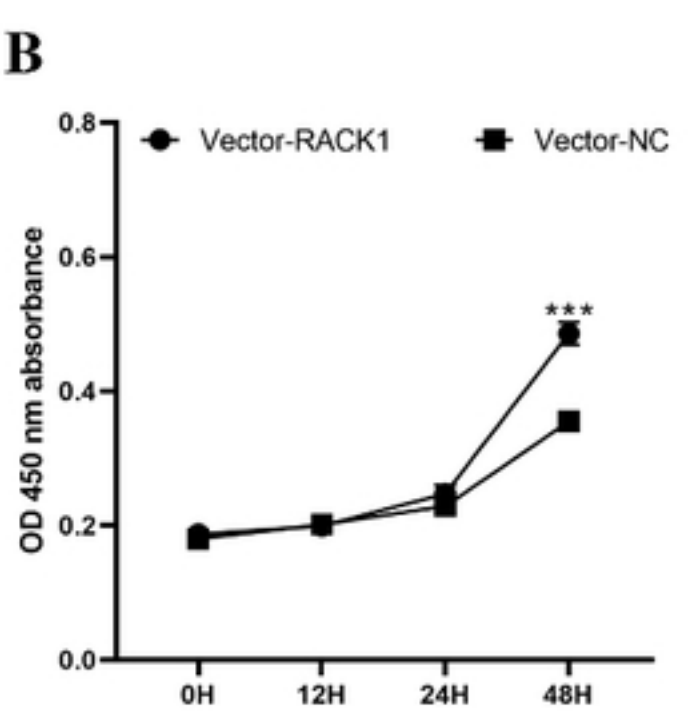
B
Vector-RACK1
Vector-NC
OD 450 nm absorbance
0.0
0.2
0.4
0.6
0.8
***
0H
12H
24H
48H

Figure

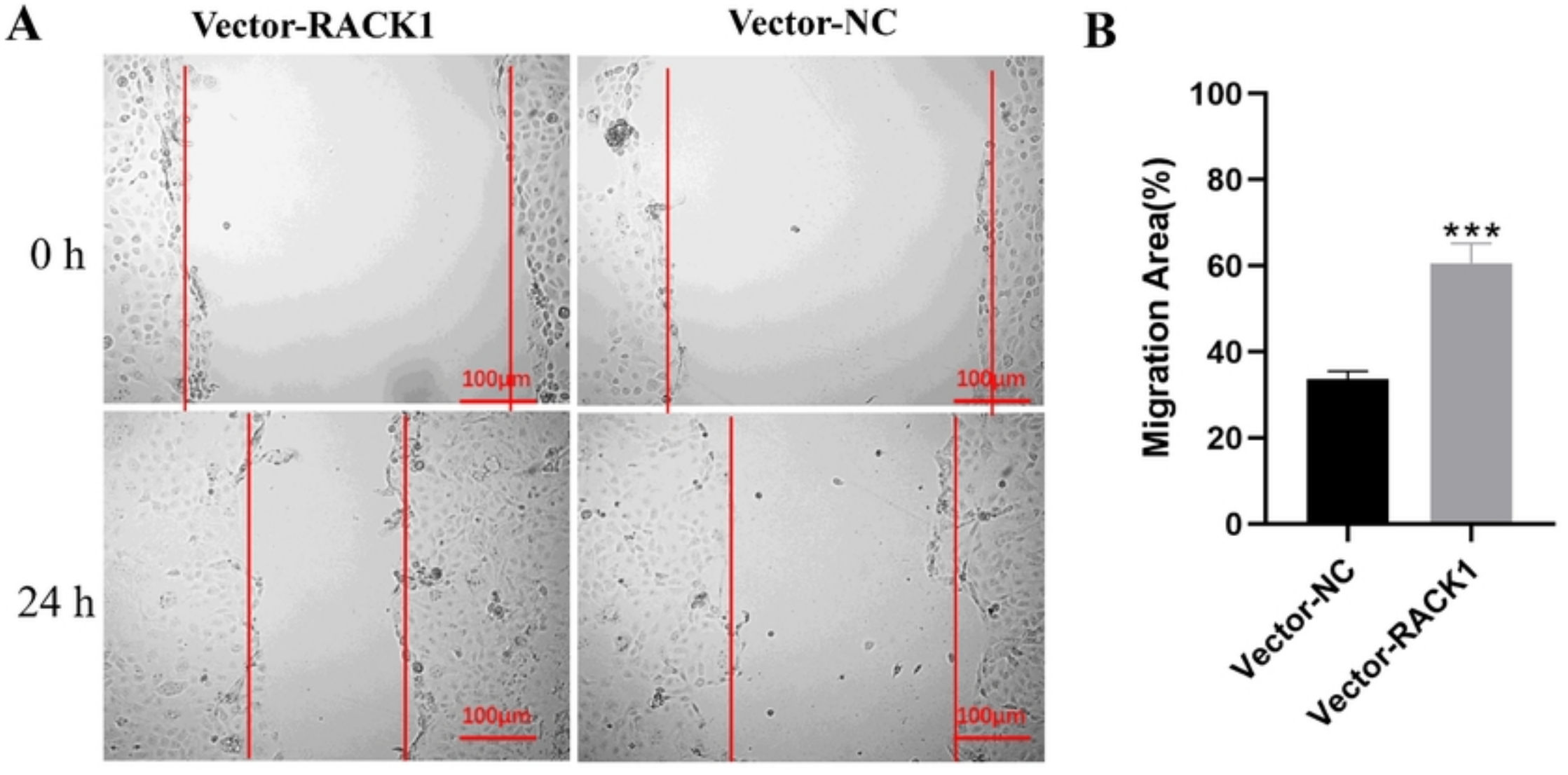
A
Vector-RACK1
Vector-NC
0 h
24 h
100μm
100μm
100μm
100μm
B
Migration Area(%)
100
80
60
40
20
0
***
Vector-NC
Vector-RACK1

Figure